Q = $Q'/\omega' l'^2$
R'_0 = jet radius, ft.
r' = radius, ft.
r = r'/l'
S' = surface velocity, V'_{rS}, ft./sec.
S = $S'/\omega' l'$
t' = time, sec.
t = $\omega' t'$, dimensionless time or rotational angle
V'_h = velocity normal to surface, ft./sec.
V'_r = radial velocity, ft./sec.
V_r = $V'_r/\omega' l'$
$\bar{V}'_0$ = average velocity at vane origin, ft./sec.
Z' = axial distance in jet

Greek Letters

ρ' = liquid density, lb.$_m$/cu. ft.
τ' = shear stress, lb.$_f$/sq. ft.
ν' = kinematic viscosity, sq. ft./sec.
μ' = viscosity, lb.$_m$/(ft.)(sec.)
ω' = angular velocity, rad./sec.

Subscripts

r, h = coordinate directions
0 = vane origin
1 = vane exit
S = surface

LITERATURE CITED

1. Duda, J. L., and J. S. Vrentas, *Chem. Eng. Sci.*, **22**, 855 (1967).
2. Goren, S. L., and S. Wronski, *J. Fluid Mech.*, **25**, 185 (1966).
3. Hallern, R. M., J. P. Johnston, and W. C. Reynolds, *ASME Paper No. 65-WA/FE-15* (1965).
4. Marshall, W. R., Jr., *CEP Monogr. Ser. No. 2*, **50** (1954).
5. Turner, H. E., and H. E. McCarthy, *AIChE J.*, **12**, 784 (1966).

Manuscript received June 9, 1969; revision received November, 1970; paper accepted November 19, 1970.

The Motion of Vapor Bubbles Growing in Uniformly Superheated Liquids

YUDA PINTO and E. JAMES DAVIS

Department of Chemical Engineering

Clarkson College of Technology, Potsdam, New York 13676

The motion of simultaneously rising and growing vapor bubbles in a uniformly superheated liquid is analyzed, and the predicted bubble velocities are shown to be in good agreement with available data. Using a quasisteady state approximation to describe the drag, and existing bubble growth theory to describe the growth rate, the equation of motion is solved for two ranges of bubble size encountered in nucleate boiling. For smaller bubbles ($R<0.04$ cm.) an analytical solution is obtained, and for larger bubbles ($R>0.07$ cm.) a numerical solution and analytical asymptotic solutions are obtained.

The motion of constant size bubbles in liquids has been widely studied, and the drag exerted on a bubble by the continuous phase has been examined both theoretically and experimentally for a wide range of bubble sizes. Considerably less information is available on the motion of growing or collapsing bubbles, although such motion is of interest in nucleate boiling, cavitation, gas bubble dissolution and chemical reaction in a liquid phase, effervescence, and other two-phase phenomena.

To predict heat and mass transfer rates associated with simultaneously growing and moving bubbles, it is necessary to have information on the translational velocity of the bubbles. It is the purpose of this paper to show that the unsteady state motion of growing bubbles can be predicted using information on the steady state motion of bubbles of constant size.

BUBBLE RISE VELOCITIES

Haberman and Morton (*1*) presented and discussed data on the terminal velocities of bubbles for a number of liquids, and their results were analyzed by Mendelson (*2*). The general behavior and ranges of interest are shown in Figure 1. The curve has been described quantitatively by Mendelson by considering the four regions indicated in the figure.

Region 1 ($R \lesssim 0.01$ cm.). Very small bubbles rise and behave like solid spheres, following Stokes' law ($N_{Re} < 1$),

but these sizes are well below the size range of interest here. Even larger bubbles in contaminated liquids behave approximately like solid spheres. Levich (3) developed the following expression for the rise velocity of a gas bubble in a pure liquid:

$$U_\infty = \frac{1}{3}\frac{gR^2}{\nu_L} \tag{1}$$

but experimental data show that the bubble rise velocity is usually lower than that predicted by Levich because of contamination of the bubble-liquid interface.

Region 2 ($0.015 \lesssim R \lesssim 0.04$ cm.). When the bubble Reynolds number ($2RU_\infty/\nu_L$) is sufficiently large ($N_{Re} > 100$), the flow field around the bubble may be approximated by potential flow, at least up to the point at which appreciable wake formation occurs. Levich (4) also analyzed the drag on a spherical bubble in this region, giving the terminal velocity as

$$U_\infty = \frac{1}{9}\frac{gR^2}{\nu_L} \tag{2}$$

Ackeret (5) obtained the drag coefficient for this range in agreement with Levich's result

$$C_D = 48/N_{Re} \tag{3}$$

For bubbles larger than about 0.04 cm., however, Equation (2) overpredicts bubble rise velocities. Harper and Moore (6) extended Levich's analysis to obtain higher order terms in the drag coefficient expression.

Region 3 ($0.07 < R < 0.3$ cm.). Bubbles with a radius $R > 0.07$ cm. begin to deviate from a perfect spherical shape, and vortex formation in the wake produces an increase in the drag. Using an equivalent radius for the bubble r_e, Peebles and Garber (7) correlated terminal velocity data in the range $0.07 < r_e < 0.3$ cm. by Equation (4):

$$U_\infty = 1.35\left(\frac{\sigma}{r_e\rho_L}\right)^{1/2} \tag{4}$$

Using a rather intuitive wave analogy, Mendelson obtained an expression for the terminal velocity of gas bubbles that is in good agreement with the data of Haberman and Morton for $0.07 \leq r_e \leq 4.0$ cm. Cole (8) found Mendelson's result to be in reasonable agreement with data for vapor bubbles rising through saturated liquids, however, the data were considerably scattered. We shall apply Equation (4) to spherical steam bubbles for which r_e may be replaced simply by the bubble radius R.

Region 4 ($R > 0.3$ cm.). Bubbles with an equivalent radius $r_e > 0.3$ assume a spherical cap shape. Haberman and Morton showed that the terminal velocity can be correlated by

$$U = 1.02\,(gr_e)^{1/2} \tag{5}$$

The vapor bubbles of interest here, which are of a size of the order of the departure radii of vapor bubbles initially growing on a solid surface, correspond to regions 1, 2, and 3. Vapor bubbles formed at a solid surface or in the bulk of a superheated liquid have been found to be spherical at moderate pressures (13 to 16), but under vacuum conditions large spherical cap bubbles are generated.

BUBBLE GROWTH

The problem of bubble growth in superheated liquids for the case of no translational motion has been analyzed by Plesset and Zwick (9), Forster and Zuber (10), Scriven (11), and others, and Bankoff (12) analyzed and reviewed the literature related to bubble growth in a uniformly superheated liquid.

Plesset and Zwick and Scriven obtained the following asymptotic expression for the bubble radius as a function of time:

$$R = 2N_{Ja}\,(3\alpha t/\pi)^{1/2} \tag{6}$$

where the Jakob number N_{Ja} is defined as

$$N_{Ja} = \frac{\rho_L C_{PL}(T_\infty - T_{sat})}{\rho_v \lambda}$$

The analysis of Forster and Zuber leads to a similar result with the constant $\sqrt{3/\pi}$ replaced by $\sqrt{\pi/4}$.

Dergarabedian (13), Hooper and Abdelmessih (14), and Kosky (15) studied stationary vapor bubble growth resulting from homogeneous nucleation in uniformly superheated water and verified the square root of time dependence of the bubble radius experimentally. Cole (16) showed that the square root of time law also applies to bubbles growing on a heated plate, but the growth constant is less than $\sqrt{3/\pi}$. In the experiments of Dergarabedian, Hooper, and Abdelmessih, and Kosky some translational bubble motion occurred because of the buoyant force acting on the bubbles, but in their analyses and interpretations they largely ignored the possible effects of translation.

More recently the effects of translational motion on heat and mass transfer associated with bubbles have been examined experimentally and theoretically. Tokuda, Yang, and Clark (17) used a potential flow model as the flow field around a bubble to analyze simultaneous translation and diffusion-controlled bubble growth or collapse. They developed small-time and large-time asymptotic expressions for the growth rate of bubbles, finding that translation can greatly increase growth rates over those predicted for stationary growing bubbles. A solution of this problem, which applies for all times, was developed by Ruckenstein and Davis (18) using a similarity transformation. They also assumed potential flow external to the bubble. For large Jakob numbers they found that the growth rate is not significantly affected by bubble rise velocities of the order of 20 cm./sec., but at small Jakob numbers such translational velocities substantially increase the growth rate compared with nonmoving bubbles. Their analysis was found to be in good agreement with data of Florschuetz et al. (19), who measured growth rates of vapor bubbles in uniformly superheated water, ethanol, and isopropanol under zero gravity and normal gravity conditions. The zero gravity results were in excellent agreement with the Scriven analysis for all times, and the normal gravity data showed good agreement with that analysis for small times.

Darby (20) measured steam bubble and Freon 113 bubble growth rates and the position of the bubbles as a function of time for bubbles nucleated heterogeneously on a solid surface. Following detachment from the nucleation site, a wire, the bubbles grew in the liquid maintained at constant superheat by infrared heating. He correlated the growth data empirically. His results are discussed further below.

In all of the above experimental studies the bubbles, except for the largest ones of Florschuetz et al. and Darby, were spherical and of sizes in the regions 1, 2, and 3 of Figure 1. Because growing bubbles are subject to varying drag forces and accelerations as they either break from a solid surface or begin growing after homogeneous nucleation in the bulk of a superheated fluid, they do not reach

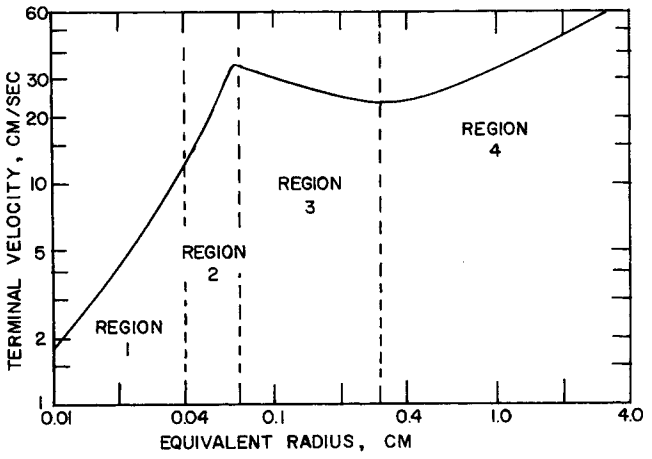

Fig. 1. Terminal velocity characteristic for bubbles.

a terminal velocity, and terminal velocity expressions for constant size bubbles do not directly apply. We shall show, however, that drag coefficient expressions strictly valid only for constant size bubbles moving at steady velocities can be used to predict the motion of accelerating and growing bubbles.

ANALYSIS

We shall consider the motion of a vapor bubble, which at time t_d departs from a solid surface where it nucleated, and then moves through a uniformly superheated liquid of large extent compared with the bubble. The equation of motion for the bubble is given by the Basset equation:

$$\frac{d}{dt}\left(\rho_v \frac{4}{3}\pi R^3 v + \frac{1}{2}\rho_L \frac{4}{3}\pi R^3 v\right) = (\rho_L - \rho_V)\frac{4}{3}\pi R^3 g - C_D \pi R^2 \frac{\rho_L v^2}{2} \quad (7)$$

The added mass term $1/2\ \rho_L\ 4/3\ \pi R^3 v$, which was first introduced by Basset (*21*) and used in most later work (*22* to *24*) on accelerating spheres, represents the momentum of liquid accelerated with the bubble. Since $\rho_L >> \rho_V$ at low and moderate pressures, the momentum of the vapor may be neglected, and the inertial effects of the added mass predominate. With this assumption Equation (7) reduces to

$$\frac{dv}{dt} + \frac{3v}{R}\frac{dR}{dt} + \frac{3}{4}C_D\frac{v^2}{R} - 2g = 0 \quad (8)$$

An examination of Equation (8) indicates that the effect of the bubble growth should be to retard the bubble motion, for with $dR/dt > 0$ the growth term $3v/R\ dR/dt$ and the drag term $3/4\ C_D\ v^2/R$ have the same sign. For a collapsing bubble $dR/dt < 0$, and the collapse should enhance the motion.

At this point it is necessary to make some assumptions about the growth rate and the drag coefficient C_D to solve Equation (8). Because of the experimental and theoretical evidence discussed above, that indicate that for sufficiently large Jakob numbers the bubble motion has no effect on the growth rate, it is reasonable to consider the bubble radius as a function of time to be given by the Plesset and Zwick equation, Equation (6). The growth rate, then, is given by

$$\frac{dR}{dt} = N_{Ja}\left(\frac{3\alpha}{\pi t}\right)^{1/2} \quad (9)$$

The choice of an appropriate drag coefficient expression is less obvious, and one analytical expression cannot be expected to be valid over a wide range of bubble sizes. Recently LeClair and Hamielec (*25*) studied the flow behavior around a solid sphere accelerating in a viscous fluid by numerically solving the complete Navier-Stokes equations for axisymmetric flow around a particle coupled to the Basset equation for the particle. Their results and previous work of Hughes and Gilliland (*26*) indicate that as the density ratio of the solid sphere to the fluid approaches infinity, the actual drag approaches the steady state drag for all ratios of the actual velocity to the terminal velocity. These results make plausible a similar approximation for growing vapor bubbles, that is, we shall assume that at any point in time the drag coefficient of the bubble is that of a bubble of constant size moving at its terminal velocity. This assumption is justified a posteriori.

The drag coefficients, then, are obtained from terminal velocity correlations for constant size bubbles. For the smaller bubbles ($R \leq 0.04$ cm.), the drag coefficient is obtained from Levich's terminal velocity expression, Equation (2), to give

$$C_D = \frac{216\nu^2}{gR^3} \qquad (R \leq 0.04 \text{ cm.}) \quad (10)$$

For the drag coefficient for larger bubbles ($R \geq 0.07$ cm.), the Peebles and Garber terminal velocity expression, Equation (4), is used to give

$$C_D = \frac{8}{3}\frac{R^2}{1.82}\frac{\rho_L g}{\sigma} \qquad (R \geq 0.07 \text{ cm.}) \quad (11)$$

Substituting Equations (10) and (11) in Equation (8) and using the Plesset and Zwick equation and Equation (9) for R and dR/dt, respectively, the equation of motion becomes

$$\frac{dv}{dt} + \frac{3}{2}\frac{v}{t} + A^*\frac{v^2}{t^2} - B = 0 \qquad (R \leq 0.04 \text{ cm.}) \quad (12)$$

and

$$\frac{dv}{dt} + \frac{3}{2}\frac{v}{t} + At^{1/2}v^2 - B = 0 \qquad (R \geq 0.07 \text{ cm.}) \quad (13)$$

where

$$A^* = \frac{81}{8}\frac{\nu_L^2}{gN_{Ja}^4\left(\frac{3\alpha}{\pi}\right)^2},$$

$$A = \frac{4N_{Ja}}{1.82}\left(\frac{3\alpha}{\pi}\right)^{1/2}\frac{\rho_L g}{\sigma},$$

and

$$B = 2g$$

Equations (12) and (13) are to be solved subject to the initial conditions at the departure of the bubble from the nucleation site. At departure the velocity of the center of the bubble is taken to be the radial velocity of the bubble wall. Thus, the initial condition is

$$\text{At} \quad t = t_d, \qquad v = v_d = \left.\frac{dR}{dt}\right|_{t_d}$$

Equation (12) has the solution

$$v = \frac{t\left\{\left(\frac{t}{c}\right)^{\phi}\left(\phi - \frac{5}{2}\right) + \phi + \frac{5}{2}\right\}}{2A^*\left[\left(\frac{t}{c}\right)^{\phi} - 1\right]} \quad (14)$$

where $\phi = \sqrt{4A^*B + 25/4}$ and c is a constant of integration obtained by applying the departure condition.

No analytical solution for Equation (13) is available, but we can obtain small-time and large-time solutions analytically, and the full equation is solved numerically.

Small-time Solution

For small times after departure from the solid surface, the drag term of Equation (13), $At^{1/2}v^2$, may be neglected, and the equation governing the motion becomes

$$\frac{dv}{dt} + \frac{3}{2}\frac{v}{t} - B = 0 \quad (15)$$

which has the solution

$$v = \frac{2}{5}Bt + \frac{C}{t^{3/2}} \quad (16)$$

where C is an integration constant determined by applying the initial condition given above.

Large-time Solution

For sufficiently large times the growth term in Equation (13), $3/2\ v/t$, can be expected to be insignificant compared with the other terms. In this case the equation reduces to

$$\frac{dv}{dt} + At^{1/2}v^2 - B = 0 \quad (17)$$

Introducing the transformation given by Murphy (27)

$$v = \frac{u'}{At^{1/2}u} \quad (18)$$

Equation (17) transforms to

$$t^2\frac{d^2u}{dt^2} - \frac{t}{2}\frac{du}{dt} - ABt^{5/2}u = 0 \quad (19)$$

which has the solution

$$u = \left(\frac{\xi}{\gamma}\right)^{3/5}\left[K_1 I_p(\xi) + K_2 I_{-p}(\xi)\right] \quad (20)$$

where $p = 3/5$, $\xi = 4/5\sqrt{AB}\,t^{5/4}$, and $\gamma = 4/5\sqrt{AB}$. Differentiating we obtain

$$\frac{du}{dt} = K_1\left[\frac{5}{4}\gamma t\left(I_{p+1} + \frac{p}{\gamma t^{5/4}}I_p\right) + \frac{3}{4}t^{-1/4}I_{-p}\right] + K_2\left[\frac{3}{4}t^{-1/4}I_p + \frac{5}{4}\gamma t\left(I_{-p+1} - \frac{p}{\gamma t^{5/4}}I_{-p}\right)\right] \quad (21)$$

Finally, the velocity is given by

$$v = \frac{\left[\frac{5}{4}\gamma t\left(I_{p+1} + \frac{p}{\gamma t^{5/4}}I_p\right) + \frac{3}{4}t^{-1/4}I_p\right]}{At^{5/4}\left(I_p + K_3 I_{-p}\right)} + \frac{K_3\left[\frac{3}{4}t^{-1/4}I_{-p} + \frac{5}{4}\gamma t\left(I_{-p+1} - \frac{p}{\gamma t^{5/4}}I_{-p}\right)\right]}{At^{5/4}\left(I_p + K_3 I_{-p}\right)} \quad (22)$$

where $K_3 = K_2/K_1$. The integration constant K_3 was determined to be 3/2 by matching Equation (22) to the numerical solution of the complete equation.

The Numerical Solution

A Runge-Kutta fourth-order integration scheme was used to solve Equation (13) numerically. Starting values of the velocity for the numerical solution are calculated from the small-time analytical solution. A time increment of 10^{-5} sec. was found to be satisfactory for good accuracy and stability of the solution.

RESULTS

Quantitative information about the time-dependent behavior of growing steam bubbles in translational motion is provided here by a parametric study of the solution of Equation (13) for various Jakob numbers. As shown by Cole (28), bubble departure radii for steam bubbles at moderate and low pressures are of the magnitude for which Equation (13) applies. The bubble velocities predicted using Equation (14) and the numerical solution of Equation (13) are also compared with Darby's data for steam bubbles and Freon 113 vapor bubbles.

Figure 2 shows the velocity versus time predictions obtained by numerical solution of Equation (13) for steam bubbles at 1 atm. growing in superheated water. Results for Jakob numbers 5, 20, and 50 are plotted in the figure, and the results of the small-time and large-time analytical solutions are also presented. The assumed departure time ($t_d = 0.004$ sec.) and the departure radii are consistent with Cole's data for steam bubbles.

The results are consistent with the qualitative observations related to Equation (8), that is, that the growth tends to reduce the acceleration that occurs immediately after departure from the solid surface. For the smallest Jakob number shown, $N_{Ja} = 5$, there is more rapid acceleration initially than for higher Jakob numbers, and the maximum velocity attained is considerably greater than for higher Jakob numbers. For $N_{Ja} = 50$ the growth rate is so large that the maximum velocity is quickly reached, and the retarding effect associated with the growth is large.

Comparison of the small-time solution, which neglects the drag, with the numerical solution indicates that the drag on the bubble is insignificant during the early part

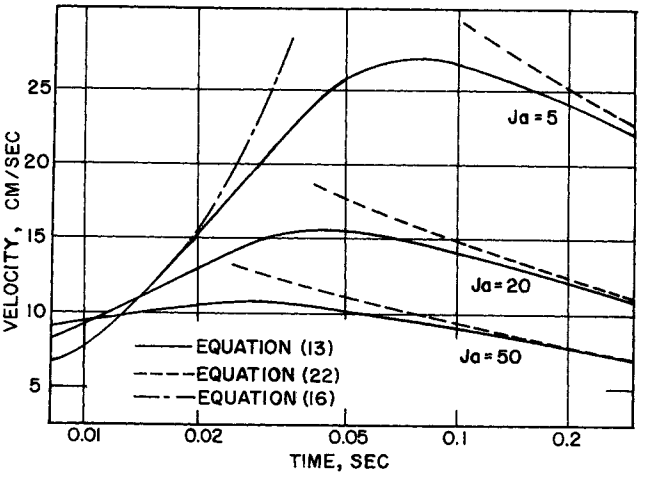

Fig. 2. The effect of bubble growth on the rise velocity predicted by numerical solution of Equation (13).

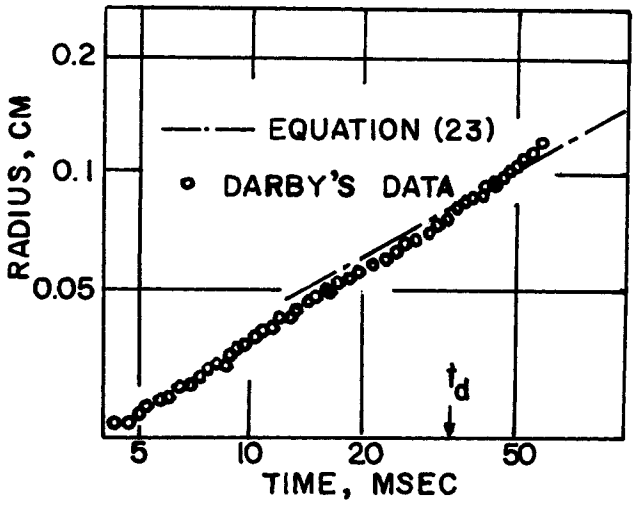

Fig. 3. A comparison of Equation (23) with Darby's steam bubble growth data of run 1.

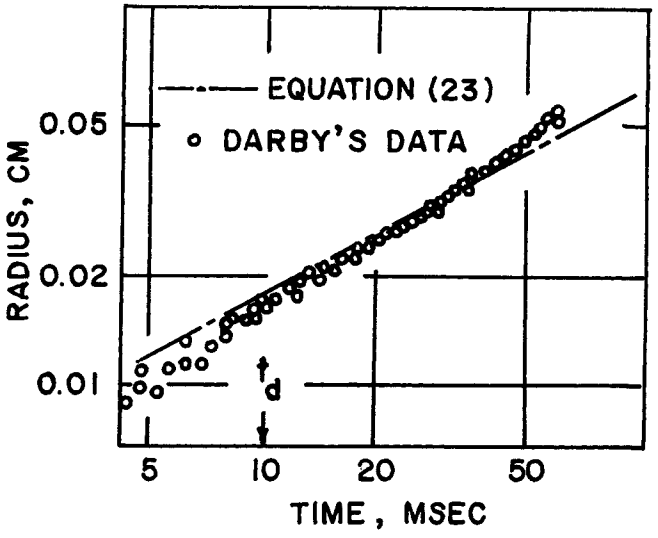

Fig. 4. A comparison of Equation (23) with Darby's Freon vapor bubble growth data for run 1A.

of the motion. The large-time solution converges on the numerical solution for earlier times as the Jakob number increases, indicating that growth rate has little retarding effect on the motion at large times.

Darby photographically measured bubble sizes and the position of the bubble relative to the nucleation site for steam bubbles and Freon 113 vapor bubbles growing in their superheated liquid phases. Uniform superheat was maintained by infrared heating. Florschuetz et al. also attempted to measure the bubble position relative to a fixed frame of reference, but they reported only bubble sizes as a function of time because of difficulties in determining the bubble velocity relative to the liquid. Only Darby has published results which can be used to test the present analysis.

Darby's experimental conditions are particularly well suited for comparison with the present analysis, for the steam bubbles involved had departure radii $R_d > 0.07$ cm., and the Freon 113 vapor bubbles were generally in the size range $0.01 < R < 0.05$ cm. Hence the steam bubble data can be compared with the solution of Equation (13), and the Freon data can be compared with Equation (14).

One problem involved with the use of Darby's results is that his growth rate data do not follow the square root of the time law. He empirically correlated his results using $R \propto t^{2/3}$. Over the limited range of sizes involved when the bubbles underwent translation after leaving the solid surface, we shall approximate the data by the following modified Plesset and Zwick equation:

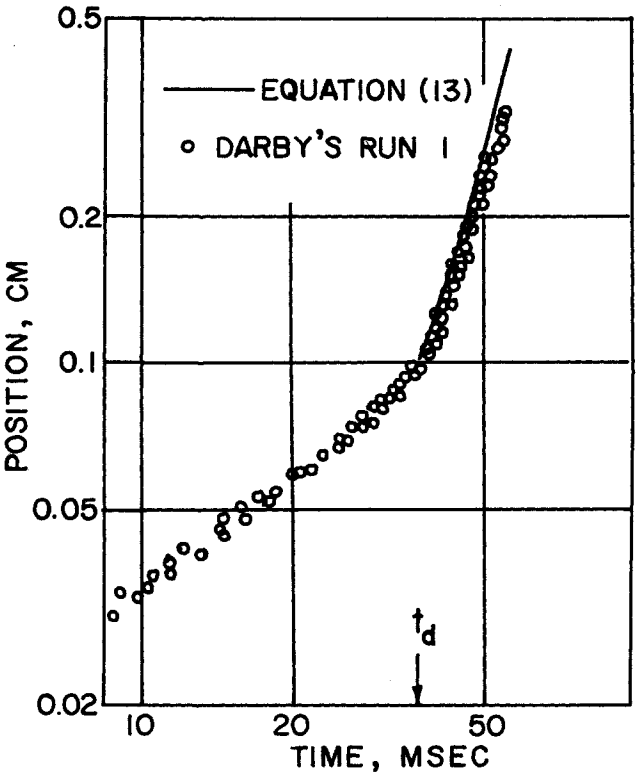

Fig. 5. A comparison of the steam bubble trajectory with the results calculated from the solution of Equation (13) for Darby's run 1.

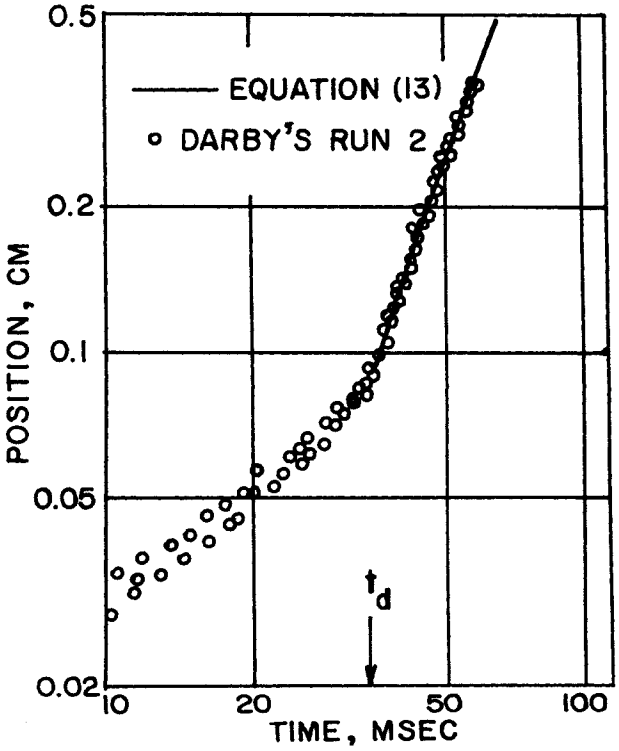

Fig. 6. A comparison of the steam bubble trajectory with the results calculated from the solution of Equation (13) for Darby's run 2.

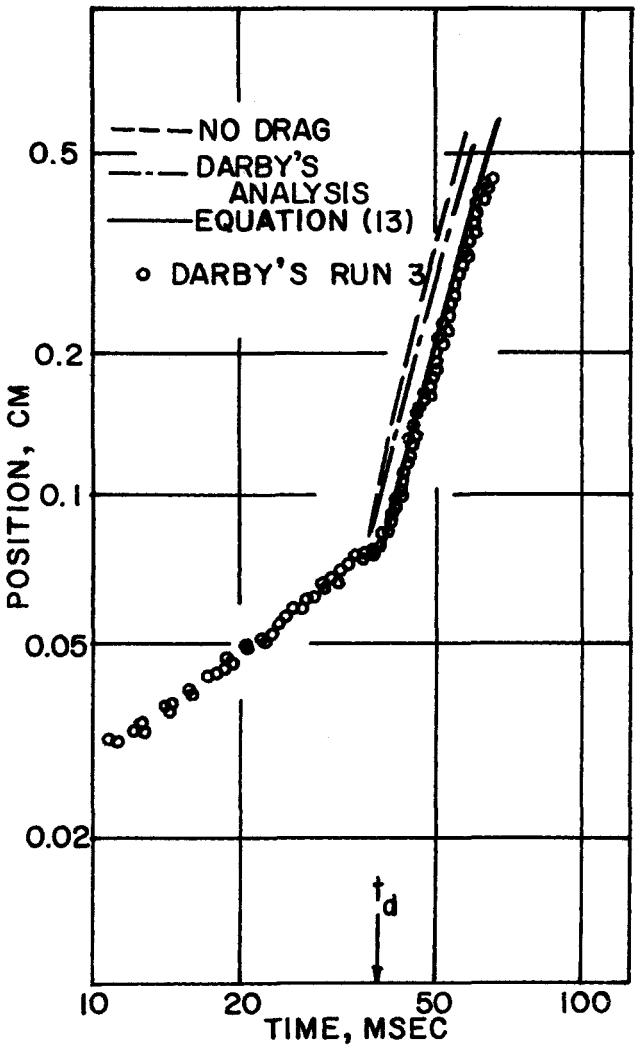

Fig. 7. A comparison among predicted and experimental trajectories for Darby's run 3.

$$R = \kappa\, 2N_{Ja} \left(\frac{3\alpha t}{\pi}\right)^{1/2} \qquad (23)$$

For the steam data κ was selected as 0.78 to fit the results, and for Freon $\kappa = 0.62$ produced a satisfactory fit of the data. Studies of the numerical solutions indicate that the particular growth law used has little effect on the results, provided that the predicted bubble radii are in reasonable agreement with the data. The analytical solutions are not valid for other growth laws, so the Plesset and Zwick form is applied as an approximation to Darby's results.

Figures 3 and 4 show typical comparisons between Equation (23) and Darby's data. The departure times are indicated on the figures. For $t < t_d$ the bubbles undergo stationary phase growth on the nucleation site. The departure times are relatively easy to obtain from Darby's plots of position versus time, for a fairly well-defined change in slope occurs at the point of departure.

The velocity predictions for typical steam bubble data of Darby are similar to the curve for $N_{Ja} = 5$ in Figure 2. The results of using Equations (13), (16), and (22) are plotted there. For these larger bubbles a maximum velocity is predicted, and for sufficiently large times the bubble growth and inertial terms have little effect on the bubble motion. Darby presented his results as the position of the bubble versus time. The theoretical velocity versus time predictions have been integrated to give the position of the bubble versus time for comparison, that is

$$S = S_0 + \int_{t_d}^{t} v\, dt \qquad (24)$$

where $S_0 = R_d$. The results are compared with Darby's steam bubble data in Figures 5 to 7, and the Freon-113 results are presented in Figures 8 and 9.

The agreement between the analysis and the experiments is remarkably good considering the limited accuracy of the assumed time dependence of the radius and the assumption that the drag coefficient can be obtained from steady state terminal velocity information. Numerical studies of the solution of Equation (8) for other growth rate expressions and for other drag coefficient relations show that the form of the growth rate expression used has relatively little effect on the predicted bubble trajectories compared with the effect of the drag coefficients used. Darby showed that if the drag is neglected the bubble trajectories predicted are in considerable error after the early rapid acceleration. He also developed an approximate solution for the bubble trajectories assuming that Stokes' law applies for the drag. Using the velocity calculated by a balance between inertial forces and the buoyancy to determine the viscous force, he integrated the equation of motion to calculate the bubble trajectories. His results for runs 3 and 1A are plotted in Figures 7 and 8 for the case of no drag and for Stokes' law drag. Similar results are obtained for the other runs. Although the approximate solution is in good agreement with the data for Freon bubbles, it significantly overpredicts the velocities for the larger steam bubbles.

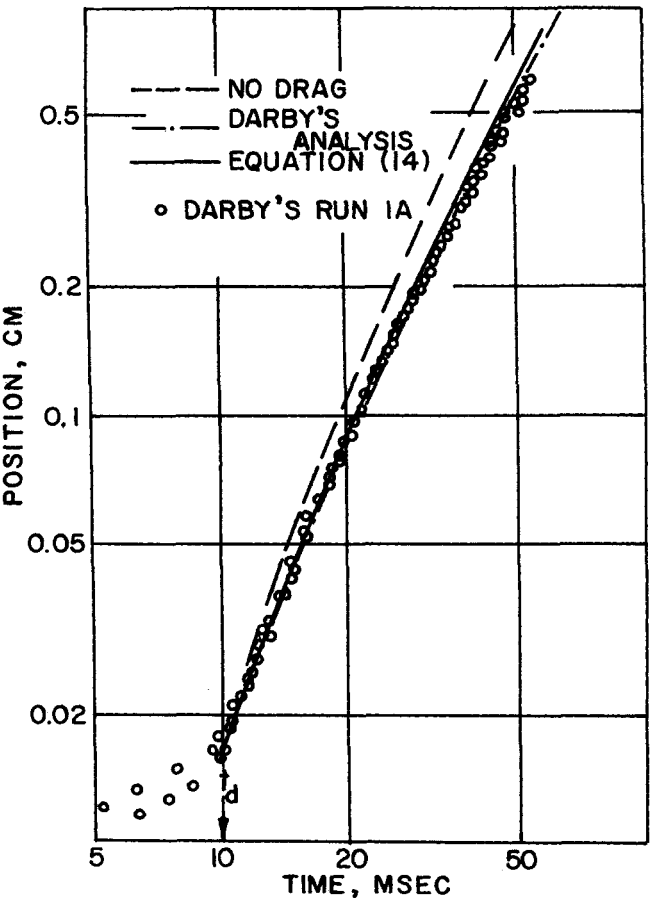

Fig. 8. A comparison among predicted and experimental trajectories for Darby's run 1A.

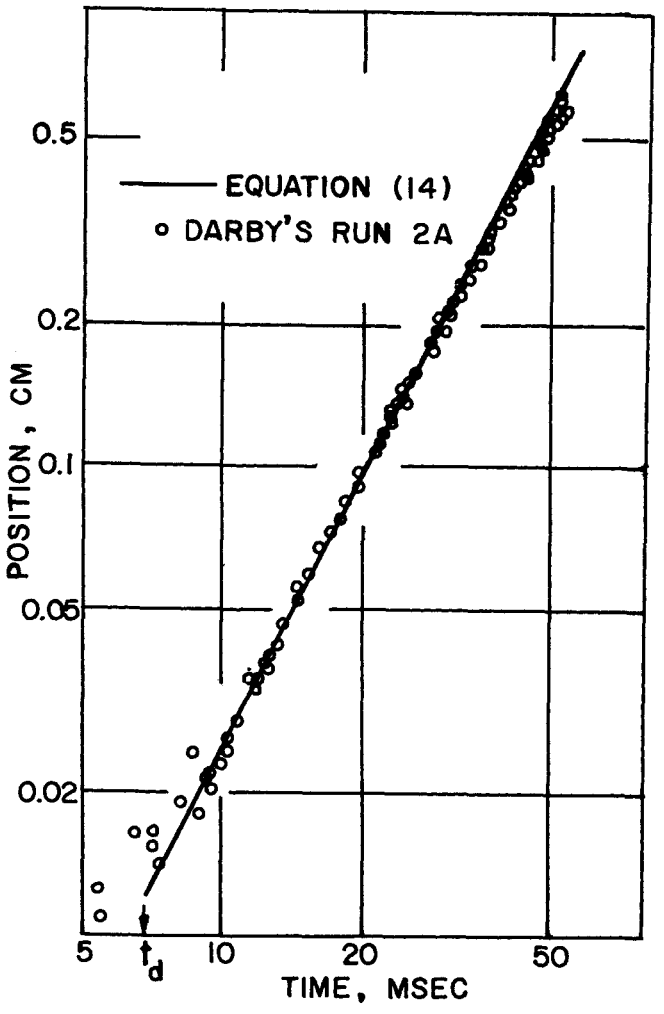

Fig. 9. A comparison of the freon bubble trajectory with the results calculated by integrating Equation (14) for Darby's run 2A.

CONCLUSIONS

The motion of simultaneously growing and accelerating vapor bubbles in a uniformly superheated liquid can be predicted using the known growth rate and drag coefficients determined from the terminal velocities of constant size bubbles.

NOTATION

A, A^* = defined parameters in Equations (12) and (13)
B = constant in Equations (12) and (13)
c, C = integration constants
C_D = drag coefficient, dimensionless
C_P = heat, capacity, cal./(g.)(°C.)
g = gravitational acceleration constant, cm./sec.^{2}
I_p, I_{-p} = modified Bessel functions of the first kind
K_1, K_2, K_3 = integration constants
N_{Ja} = Jakob number, dimensionless
N_{Re} = bubble Reynolds number
r_e = equivalent radius, cm.
R = bubble radius, cm.
S = position of bubble, cm.
t = time, sec.
T = temperature, °C.
u = transformation variable
U_∞ = terminal velocity, cm./sec.
v = bubble velocity, cm./sec.

Greek Letters

α = thermal diffusivity, sq.cm./sec.
γ = defined parameter in Equation (20)
κ = defined constant in Equation (23)
λ = heat of vaporization, cal./g
ν = kinematic viscosity, sq.cm./sec.
ξ = independent variable in Equation (20)
ρ = density, g./cu.cm.
σ = surface tension, dynes/cm.
ϕ = defined parameter in Equation (14)

Subscripts

d refers to a departure condition
L refers to the liquid phase
sat refers to the saturation temperature
V refers to the vapor phase
∞ refers to a property at great distance from the bubble interface

LITERATURE CITED

1. Haberman, W. L., and R. K. Morton, *David Taylor Model Basin, NR 715-102* (1953).
2. Medelson, H. D., *AIChE J.*, **13**, 250 (1967).
3. Levich, V. G., "Physicochemical Hydrodynamics," Prentice Hall, Englewood Cliffs, N. J. (1962).
4. Levich, V. G., *Zh., Eksp. Tevret. Fiz.*, **19**, 18 (1949).
5. Ackeret, J., *Z. Angew. Math. Phys.*, **3**, 259 (1952).
6. Harper, J. F., and D. W. Moore, *J. Fluid Mech.*, **32**, 367 (1968).
7. Peebles, F. N., and H. J. Garber, *Chem. Eng. Progr.*, **49**, 88 (1953).
8. Cole, R., *AIChE J.*, **13**, 403 (1967).
9. Plesset, M. S., and S. A. Zwick, *J. Appl. Phys.*, **25**, 493 (1954).
10. Forster, A. K., and N. Zuber, *ibid.*, 474 (1954).
11. Scriven, L. E., *Chem. Eng. Sci.*, **10**, 1 (1959).
12. Bankoff, S. G., "Advances in Chemical Engineering," Vol. 6, Academic Press, New York (1966).
13. Dergarabedian, P., *J. Appl. Mech.*, **20**, 537 (1953).
14. Hooper, F. C., and A. H. Abdelmessih, *Proc. Third Intern. Heat Transfer Conf.*, **4**, 44 (1966).
15. Kosky, P. G., *Chem. Eng. Sci.*, **23**, 695 (1968).
16. Cole, R., Ph.D. thesis, Clarkson Coll. Technol., Potsdam, N. Y (1965).
17. Tokuda, N., W. J. Yang, and J. A. Clark, *J. Heat Transfer*, **90**, 371 (1968).
18. Ruckenstein, E., and E. J. Davis, *Intern. J. Heat Mass Transfer*, **14**, 939 (1971).
19. Florschuetz, L. W., C. L. Heney, and A. R. Khan, *ibid.*, **12**, 1465 (1969).
20. Darby, R., *Chem. Eng. Sci.*, **19**, 39 (1964).
21. Basset, A. B., *Phil. Trans. Roy. Soc. London*, **17**, 43 (1888).
22. Brush, L. M., H. W. Ho, and B. C. Yen, *J. Hydraulics Div. ASCE*, **90**, 149 (1964).
23. Odar, F., *J. Fluid Mech.*, **25**, 591 (1966).
24. Hjelmfelt, A. T., and L. F. Mockros, *J. Eng. Mech. Div. ASCE*, **93**, 87 (1967).
25. LeClair, B. P., and A. E. Hamielec, reprint from the Fluid Dynamics Symp., McMaster Univ., Hamilton, Ontario (Aug. 1970).
26. Hughes, R. R., and E. R. Gilliland, *Chem. Eng. Progr.*, **48**, 497 (1952).
27. Murphy, G. M., "Ordinary Differential Equations and Their Solutions," D. Van Nostrand, Princeton, N.J. (1960).
28. Cole, R., *AIChE J.*, 13, 779 (1967).

Manuscript received March 22, 1971; revision received April 16, 1971; paper accepted April 20, 1971.